Scalar warm inflation in holographic cosmology

Zahra Bouabdallaoui,[1,*] Ahmed Errahmani,[1,†] Mariam Bouhmadi-López,[2,3,‡] and Taoufik Ouali[1,§]

[1]*Laboratory of Physics of Matter and Radiation, University of Mohammed first, BP 717, Oujda, Morocco*
[2]*Department of Physics University of the Basque Country UPV/EHU. P.O. Box 644, Bilbao 48080, Spain*
[3]*IKERBASQUE, Basque Foundation for Science, Bilbao 48011, Spain*

(Received 23 November 2020; revised 6 January 2022; accepted 18 January 2022; published 9 February 2022)

We consider warm inflation in the context of holographic cosmology. The weak and the strong dissipative regime are analyzed in the slow-roll approximation and within what is known as intermediate inflation. For an appropriate choice of the equation of state, the intermediate inflation is not only an exact solution in general relativity, but it is also in the holographic setup considered in this paper. Within this approach several dissipative and physically relevant functions are considered. We constrain our model using the latest Planck data. We conclude that three of the models analyzed are consistent with Planck data for some ranges of the model parameters. However, one of them is ruled out by the observations.

DOI: 10.1103/PhysRevD.105.043513

I. INTRODUCTION

The inflationary paradigm was proposed to sort out several shortcomings of the standard big bang theory [1–6]. In addition, this paradigm reproduces correctly the distribution of the large scale structure [7–11] and the observed anisotropy of the cosmic microwave background [12–16]. The zoo of the inflationary models is quite wild and many models are consistent with the current observations. Therefore, it would be quite interesting to have some approach that alleviate such a degeneracy [17–21]. Within the inflationary scenario with a slow roll approach, two roads can be taken. On the one hand, in the cold inflationary scenario, the inflaton does not interact with its environment and the reheating of the Universe takes place at the end of inflation when the scalar field reach the bottom of the potential and starts oscillating. However, this kind of approach might face some fine-tuning problems and the reheating problem itself. Furthermore, the latest Planck data ruled out many forms of inflaton potentials, including, for instance, the quadratic and quartic potentials, both well motivated from a particle physics perspective. On the other hand, there is the warm inflationary scenario, where the radiation production occurs gradually as the Universe inflates through the dissipation of the inflaton field into a thermal radiation [22,23]. In addition, initial density fluctuations (the seeds of the large scale structure) is produced during the warm inflationary era; i.e., the fluctuation of the inflaton field is due to a thermal process rather than to a quantum one as in cold inflation [24–28]. This thermal process affect deeply the background and the perturbative results of the inflationary dynamics [29,30].

Furthermore, cold and warm inflation have been well studied in the framework of an effective approach to quantum gravity. Indeed, for example in extra-dimensions models, motivated by superstring theory [31,32] such as braneworld models where matter is considered to be confined in a 3-brane while gravity can propagate in the bulk, have been a natural arena for inflation. In addition, warm inflation has been analyzed in a modified theory of gravity, like braneworlds [33–42] and in loop quantum cosmology [43–47]. We would to remember that the Randall and Sundrum model [48] is extremely well motivated and can be used as the main setup of the AdS/CFT correspondence. We recall that the AdS/CFT correspondence, conjectured by Maldacena [49], consists in describing the five-gravitational theory as a conformal field theory on the 4D boundary space-time. This duality can be seen as an holographic approach. The effect of the holographic picture on cold inflation has been analyzed in [50,51] by a conformal field theory on its four-dimensional boundary space-time. Previous study of the effect of this holographic picture on cold inflation scenario might be found in Refs. [50,51], and its extension by a nonminimal coupling to the induced gravity by means of the dynamical system and the modifications of the amplitude of the primordial perturbation in [52,53]. Recently, we have studied a nonminimal coupling Higgs inflation in this context [54].

In this paper, we study warm inflation within an holographic view point in order to complete our previous study [51] and to see how well is warm inflation supported within the holographic picture. In this context, we consider a well-known form of the scale factor and named as intermediate

*zahraandto@hotmail.com
†ahmederrahmani1@yahoo.fr
‡mariam.bouhmadi@ehu.es
§ouali1962@gmail.com

inflation. This kind of model was already studied in general relativity and in a modified theory of gravity [55–60].

The outline of the paper is as follow. In Sec. II, we construct the main formulas of warm inflation in the context of the holographic duality. In Sec. III, we show how the intermediate inflation occurs according to the holographic setup. In Sec. IV, we review the main formulas used in warm inflation at the perturbative level. In Secs. V and VI we consider the case of the weak and the strong dissipation regime respectively. In these sections, we compute the main parameters of these regime in terms of the holographic parameter and of the perturbation parameters. We conclude our paper in Sec. VII.

II. HOLOGRAPHIC WARM INFLATION

In the AdS/CFT correspondence, the Friedmann equation is modified as [50,61]

$$H^2 = \frac{2\kappa\rho_c}{3}\left(1+\epsilon\sqrt{1-\frac{\rho}{\rho_c}}\right), \tag{2.1}$$

where $\kappa = \hat{m}_p^{-2} = 8\pi m_p^{-2}$ and m_p is the four-dimensional Planck mass, ρ is the total energy density, $\rho_c = 3\hat{m}_p^4/8c$, and $c = \hat{m}_p^6/M^6$ is the conformal anomaly coefficient which is defined as the ratio between the four-dimensional Planck mass and the five-dimensional mass M. At the low-energy limit, $\rho \ll \rho_c$, and for the branch $\epsilon = -1$ the standard form of the Friedmann equation can be recovered. In the following only this branch will be considered. In warm inflation, we will consider that the Universe is filled with a self-interacting scalar field with energy density ρ_ϕ and a radiation energy density ρ_γ.

The conservation law of the total energy density $\rho = \rho_\phi + \rho_\gamma$ reads

$$\dot{\rho}_\phi + 3H(\rho_\phi + p_\phi) + \dot{\rho}_\gamma + 4H\rho_\gamma = 0. \tag{2.2}$$

The dynamical equations for the energies densities, ρ_ϕ and ρ_γ, in warm inflation are described, respectively, by [23]

$$\dot{\rho}_\phi + 3H(\rho_\phi + p_\phi) = -\Upsilon\dot{\phi}^2, \tag{2.3}$$

$$\dot{\rho}_\gamma + 4H\rho_\gamma = \Upsilon\dot{\phi}^2, \tag{2.4}$$

where a dot means derivative with respect to the cosmic time. The positive dissipation factor, Υ, is responsible for the reheating the Universe through the decay of the scalar field ϕ. Several phenomenological expression for the dissipation term $\Upsilon\dot{\phi}^2$ are given in the literature [62–68].

Following Refs. [66,67], we consider the general form of the dissipative coefficient, given by

$$\Upsilon(\phi, T) = C_\phi \frac{T^m}{\phi^{m-1}}, \tag{2.5}$$

where m is an integer and C_ϕ is associated to the dissipative microscopic dynamics. Different expressions for the dissipation coefficient, i.e., different choices of values of m, have been analyzed in [66–68]. In this paper, we will discuss the following cases

(i) $m = -1$ which corresponds to the dissipation rate of the nonsupersymmetric model [63,64].
(ii) $m = 0$ in which the dissipation coefficient represents an exponentially decaying propagator in the high temperature regime. A dissipation coefficient which depends only on the scalar field was first considered in warm inflation in [69].
(iii) $m = 1$ corresponds to the high temperature regime [29,70–72].
(iv) $m = 3$ is motivated by a supersymmetric model [29,67,73], a minimal warm inflation [74–76], a quantum field theory model of inflation [77], and through axion inflation [78]. Furthermore, this case is used in other contexts such as in a hilltop model [79], in a stochastic approach [80], in a potential with an inflection point [81] and in runway potentials [82]. By using a sphaleron rate in a non-Abelian gauge fields [74], a Chern-Simons diffusion rate in a minimal warm inflation [75] and in the Dirac-Born infeld [76], the authors show that the dissipative coefficient in the case $m = 3$ does not depend on the inflaton fields as in Eq. (2.5).

The energy density, ρ_ϕ, and the pressure, p_ϕ, of the standard scalar field can be written as

$$\rho_\phi = \frac{\dot{\phi}^2}{2} + V(\phi), \qquad p_\phi = \frac{\dot{\phi}^2}{2} - V(\phi), \tag{2.6}$$

where $V(\phi)$ represents the effective potential.

By introducing the dimensionless dissipation parameter Q, defined as

$$Q \equiv \frac{\Upsilon}{3H}, \tag{2.7}$$

Eq. (2.3) can be rewritten as

$$\dot{\rho}_\phi = -3H\dot{\phi}^2(1+Q). \tag{2.8}$$

We will consider two dissipative regimes on this paper. The strong dissipative one characterized by $Q \gg 1$ and the weak dissipative one in which $Q \ll 1$.

At the epoch of warm inflation it is safe to assume that the energy density of the scalar field is the dominant component of the cosmic fluid ($\rho_\phi \gg \rho_\gamma$) [23,24,27]. Therefore, the effective Friedmann Eq. (2.1) reduces to

$$H^2 \approx \frac{2\kappa\rho_c}{3}\left(1-\sqrt{1-\frac{\rho_\phi}{\rho_c}}\right), = \frac{2\kappa\rho_c}{3}\left(1-\sqrt{1-\frac{\frac{\dot{\phi}^2}{2}+V(\phi)}{\rho_c}}\right), \tag{2.9}$$

Furthermore, by combining Eq. (2.8) and the derivative of Eq. (2.9), one can show that

$$\dot{\phi}^2 = [\dot{\phi}^2]_{\rm std} G, \tag{2.10}$$

where

$$[\dot{\phi}^2]_{\rm std} = -\frac{2\dot{H}}{\kappa(1+Q)} \tag{2.11}$$

and

$$G = 1 - \frac{3H^2}{2\kappa\rho_c} \tag{2.12}$$

are the kinetic energy density of the scalar field in standard warm cosmology [83] and the correction term characterizing the effect of AdS/CFT correspondence, respectively.

We can notice that at the low energy limit, ($\rho \ll \rho_c$), the correction term reduces to one and the standard expression of the scalar field is recovered.

We suppose that during warm inflation the radiation production is quasistable, i.e., $\dot{\rho}_\gamma \ll 4H\rho_\gamma$ and $\dot{\rho}_\gamma \ll \Upsilon\dot{\phi}^2$ [23,24,27]. The combination of Eqs. (2.4) and (2.10) yields

$$\rho_\gamma = [\rho_\gamma]_{\rm std} G, \tag{2.13}$$

where $[\rho_\gamma]_{\rm std}$ is the radiation energy density in standard warm inflation [83] expressed as

$$[\rho_\gamma]_{\rm std} = -\frac{\Upsilon\dot{H}}{2\kappa H(1+Q)}. \tag{2.14}$$

Furthermore, the energy density of radiation is related to the temperature as [84]

$$\rho_\gamma = C_\gamma T^4, \tag{2.15}$$

where $C_\gamma = \pi^2 g_*/30$ and g_* characterize the number of relativistic degrees of freedom. Substituting Eq. (2.15) into Eq. (2.13), the temperature of the thermal bath T can be written as

$$T = [T]_{\rm std} G^{\frac{1}{4}}, \tag{2.16}$$

where $[T]_{\rm std}$ is the temperature in standard warm inflation [83]

$$[T]_{\rm std} = \left[-\frac{\Upsilon\dot{H}}{2\kappa C_\gamma H(1+Q)}\right]^{\frac{1}{4}}. \tag{2.17}$$

Substituting Eq. (2.16) in (2.5), we get that

$$\Upsilon^{\frac{4-m}{4}} = C_\phi \left[\frac{1}{2\kappa C_\gamma}\right]^{\frac{m}{4}} \phi^{1-m} \left[-\frac{\dot{H}}{H}\right]^{\frac{m}{4}} (1+Q)^{-\frac{m}{4}} G^{\frac{m}{4}}. \tag{2.18}$$

At low energy limit, ($\rho \ll \rho_c$), the standard expression [83] of Eq. (2.18) is recovered.

Furthermore, by solving Eq. (2.9) for the scalar density and using simultaneously Eq. (2.10), we find the effective potential

$$V(\phi) = \frac{3H^2}{2\kappa}(1+G) + \frac{\dot{H}}{\kappa(1+Q)}\left(1+\frac{3}{2}Q\right)G. \tag{2.19}$$

At the low energy limit, Eq. (2.19) recovers the expression of standard warm inflation [83].

III. INTERMEDIATE INFLATION

In order to illustrate our purpose, we will focus on the intermediate scenario of inflation [30,55–59] in which an exact solution can be obtained. Nevertheless, exact solutions can also be found for power law expansion of the Universe [85] and in the de Sitter inflationary scenario [5]. In the intermediate scenario of inflation, the scale factor obeys the following expression [30,55–59]

$$a(t) = a_I \exp(At^f), \tag{3.1}$$

where the two constants f and A satisfy the conditions $0 < f < 1$ and $0 < A$, respectively. The intermediate inflation model may be derived from an effective theory at low dimensions of a fundamental string theory. Therefore, the study of the intermediate inflationary model is motivated by string/M theory. In this scenario, the cosmic expansion evolves slower than the standard de Sitter model, $a(t) \propto \exp(H_I t)$ and faster than power law inflation ($a \propto t^p$, $p > 1$).

The intermediate scenario of inflation is still an exact solution in our holographic setup. Indeed, an appropriate choice of the equation of state of the form

$$\rho + p = \gamma\rho_c \sqrt{1-\frac{\rho}{\rho_c}}\left[\left(1-\sqrt{1-\frac{\rho}{\rho_c}}\right)\right]^\lambda, \tag{3.2}$$

for $\lambda > 1$ and $\gamma > 0$ reproduces this intermediate paradigm. For $\lambda = 1$ and $\rho \ll \rho_c$, we recover the standard Friedmann equation and the barotropic equation of state $p = (\gamma - 1)\rho$. The equation of state (3.2) implies that while the weak energy conditions [86] are satisfied, the strong energy condition ($\rho + 3p \geq 0$) is violated for a sufficiently small energy density and for $\lambda > 1$. The violation of the strong energy condition assure that the acceleration of the Universe takes place.

With the help of Eq. (2.1) and the conservation of the total energy density

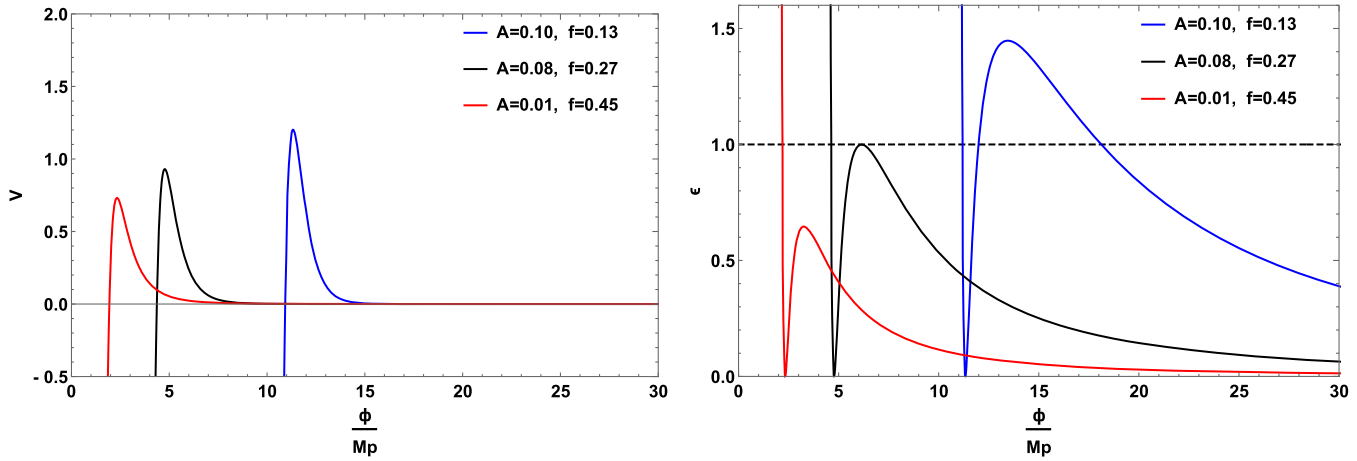

FIG. 1. Plot of the potential (left curve) and the slow roll parameter (right curve) in the weak dissipative regime for ($A = 0.01$, $f = 0.45$), ($A = 0.08$, $f = 0.27$), and ($A = 0.1$, $f = 0.13$). The horizontal dashed line (right curve) corresponds to $\epsilon = 1$.

$$\dot{\rho} + 3H(\rho + p) = 0, \tag{3.3}$$

where $\rho = \rho_\phi + \rho_\gamma$ and $p = p_\phi + p_\gamma$ are the energy density and the pressure, respectively, a straightforward calculus leads to the intermediate inflation given by Eq. (3.1).

On the other hand, the dimensionless slow-roll parameters are given by

$$\epsilon \equiv -\frac{\dot{H}}{H^2} = \frac{1-f}{Aft^f}, \tag{3.4}$$

$$\eta \equiv -\frac{\ddot{H}}{2H\dot{H}} = \frac{2-f}{2Aft^f}. \tag{3.5}$$

In order to estimate the scale where the perturbations cross the Hubble radius, we need to define the end of inflation, i.e., $\epsilon = 1$. According to the behavior of the potential [see Eq. (2.19)], a description of how inflation ends in our model requires a deeper analysis which is out of the scope of this paper. However, to illustrate our purpose, we have plotted, in Figs. 1 and 2, the potential V and the first slow roll parameter ϵ for the couple of parameters (A, f). The weak dissipative regime is illustrated in Fig. 1 for $(A = 0.01,\ f = 0.45)$, $(A = 0.08,\ f = 0.27)$, and $(A = 0.1,\ f = 0.13)$, and the strong dissipative regime is illustrated in Fig. 2 for $(A = 0.1,\ f = 0.2)$, $(A = 0.1,\ f = 0.12)$, and $(A = 0.1,\ f = 0.06)$. We notice from Fig. 1 that the slow roll parameter is always less than 1 and its violation cannot stop inflation, in the decreasing branch of the potential, in the cases $(A = 0.01,\ f = 0.45)$ and $(A = 0.1,\ f = 0.2)$ for weak and strong dissipative regime, respectively. In this case, a modification of the model by adding a new a parameter ϕ_{end} may trigger the stop of the intermediate inflation [87]. In the case of $(A = 0.1,\ f = 0.13)$ and $(A = 0.1,\ f = 0.06)$, the slow roll parameter is always higher than 1 and the intermediate inflation may occur between values of the scalar field where

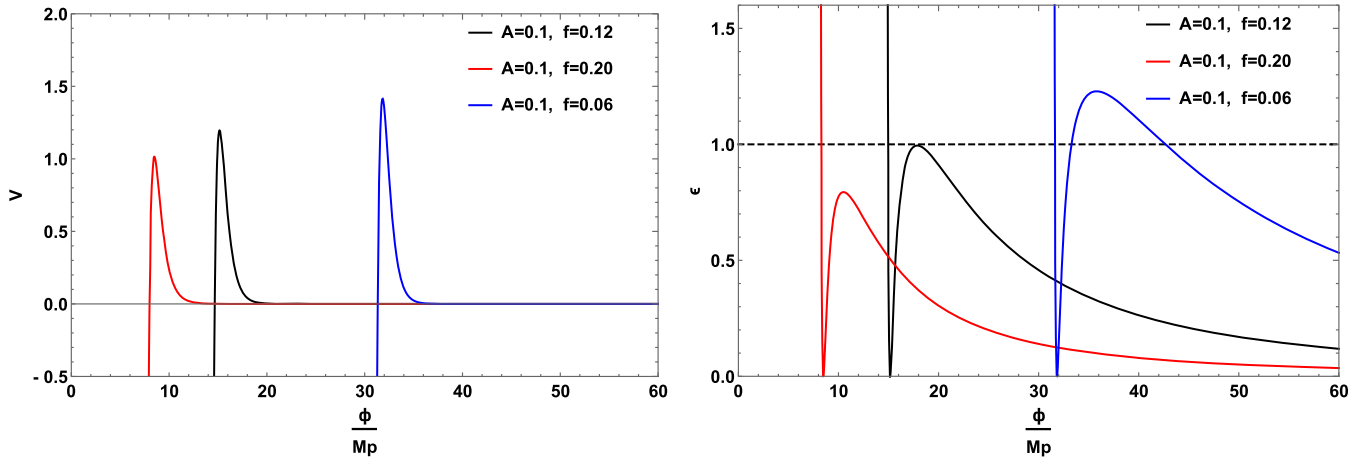

FIG. 2. Plot of the potential (left curve) and the slow roll parameter (right curve) in the strong dissipative regime for ($A = 0.1$, $f = 0.2$), ($A = 0.1$, $f = 0.12$), and ($A = 0.1$, $f = 0.06$). The horizontal dashed line (right curve) corresponds to $\epsilon = 1$.

the scalar field reaches the maximum of the potential and the scalar field value at which $\epsilon = 1$ (first solution) for weak and strong dissipative regimes, respectively. In the last case, the intermediate inflation may also occur between values of the scalar field at which $\epsilon = 1$ (the second solution) and infinite values of the scalar field.

Furthermore, the number e-folds N is given by

$$N = \int_{t_k}^{t_{\rm end}} H dt = A(t^f_{\rm end} - t^f_k), \tag{3.6}$$

where t_k and $t_{\rm end}$ are the cosmic time at the horizon crossing and at the end of inflation, respectively. By equating Eq. (3.4) to unity, we obtain $t_{\rm end} = (\frac{1-f}{Af})^{\frac{1}{f}}$, and Eq. (3.6) gives us the cosmic time at the horizon crossing

$$t_k \doteq I(N) = \left(\frac{1 - f(N+1)}{Af}\right)^{\frac{1}{f}}. \tag{3.7}$$

IV. PERTURBATIONS AND WARM INFLATION

Warm inflation not only affects the background parameters but can also modify those at the perturbative level as the scalar perturbations; though, the tensor perturbations remain unchanged. The general idea for the perturbations in warm inflation being of thermal origin were given in [23–27]. However, the most relevant works with the modern notation in which the fluctuations in the scalar field are mainly originated from thermal fluctuation rather than quantum fluctuations during warm inflation can be found in [63,88–90].

In order to study the cosmological perturbations, we consider the scalar perturbations of a Friedmann-Lemaître-Robertson-Walker background in the longitudinal gauge. Therefore, the perturbed metric reads

$$ds^2 = -(1 + 2\Phi)dt^2 + a^2(t)(1 - 2\Phi)\delta_{ij}dx^i dx^j, \tag{4.1}$$

where $a(t)$ is the scale factor, $\Phi(t, x)$ is the scalar perturbation. Furthermore, the dissipative coefficient depends explicitly, in general, on the temperature and on the inflaton field as given in Eq. (2.5). This dependence modifies the set of the perturbative equations. In fact, the amplitude of the scalar perturbation of the inflaton field will be enhanced by a correction factor. These modifications appear not only because of the scalar perturbations of the background metric but also due to the existence of a dissipative coefficient in the conservation of the energy momentum tensor through

$$\delta\Upsilon = \frac{\partial\Upsilon}{\partial T}\delta T + \frac{\partial\Upsilon}{\partial\phi}\delta\phi. \tag{4.2}$$

As we will notice in the next paragraph, this modification will affect strongly the amplitude of the scalar spectrum. This treatment has been already studied in literatures, e.g., [67,88,89,91,92]. In the next paragraph, we introduce the amplitude of the scalar perturbation of the inflaton field as evaluated at the horizon crossing. Like we did previously, we assume that the perturbations will not be highly affected by the holographic approach effect. Therefore, we assume that the amplitude of the scalar perturbation is given by [82,88,91–93]

$$P_R = \left(\frac{H^2}{2\pi\dot{\phi}}\right)^2 \left(1 + 2n + \frac{2\sqrt{3}\pi Q}{\sqrt{3 + 4\pi Q}}\frac{T}{H}\right) F(Q), \tag{4.3}$$

where the coefficient n denotes the statistical distribution for the inflaton field. By assuming that the inflaton is in thermal equilibrium with the radiation bath, n behaves like a Bose-Einstein distribution. The function $F(Q)$ describes the coupling between the inflaton field and radiation. Its expression is obtained numerically by resolving the systems of perturbations equations for warm inflation [67,72,88,90]. We will specify its numerical fit in the strong dissipative regime for each value of the dissipative coefficient. From Eqs. (2.10), (2.11), and (2.16), Eq. (4.3) can be rewritten as

$$P_R = \frac{1}{4\pi^2}H^4\left[-\frac{2\dot{H}}{\kappa(1+Q)}\right]^{-1} \times G^{-1}\left(1 + 2n + \frac{2\sqrt{3}\pi Q}{\sqrt{3 + 4\pi Q}}\frac{T}{H}\right)F(Q), \tag{4.4}$$

where

$$\frac{T}{H} = \left[-\frac{\Upsilon\dot{H}}{2\kappa C_\gamma H(1+Q)}\right]^{\frac{1}{4}} H^{-1}G^{\frac{1}{4}}, \tag{4.5}$$

and the combination of Eqs. (2.7) and (2.18) give

$$Q[1+Q]^{\frac{m}{4-m}} = \frac{1}{3H}C_\phi^{\frac{4}{4-m}}\left[\frac{1}{2\kappa C_\gamma}\right]^{\frac{m}{4-m}}\phi^{4\frac{1-m}{4-m}}\left[-\frac{\dot{H}}{H}\right]^{\frac{m}{4-m}}G^{\frac{m}{4-m}}, \tag{4.6}$$

which can be rewritten in term of the parameters of the intermediate inflation, Eq. (3.1), as

$$P_R = \frac{A^4 f^4}{4\pi^2}\left[\frac{2Af(1-f)}{\kappa(1+Q)}\right]^{-1} I(N)^{3f-2}(1 - S(I(N))^{2f-2})^{-1}\left(1 + 2n + \frac{2\sqrt{3}\pi Q}{\sqrt{3 + 4\pi Q}}\frac{T}{H}\right)F(Q), \tag{4.7}$$

$$\frac{T}{H}=\frac{1}{Af}\left[\frac{3Af(1-f)}{2\kappa C_\gamma}\frac{Q}{1+Q}\right]^{\frac{1}{4}}I(N)^{\frac{2-3f}{4}}(1-S(I(N))^{2f-2})^{\frac{1}{4}}, \tag{4.8}$$

$$Q[1+Q]^{\frac{m}{4-m}}=\frac{C_\phi^{\frac{4}{4-m}}}{3Af}\left[\frac{(1-f)}{2\kappa C_\gamma}\right]^{\frac{m}{4-m}}\phi^{4\frac{1-m}{4-m}}I(N)^{-f+\frac{2m-4}{m-4}}[1-S(I(N))^{2f-2}]^{\frac{m}{4-m}}. \tag{4.9}$$

where the quantities $S=3A^2f^2/2\kappa\rho_c$ and $I(N)$ are given by Eq. (3.7).

In the next section, we will examine separately the weak dissipative regime and the strong one. In the weak dissipative case, we will approximate the function $F(Q)$ to be equal to one while for the strong dissipative regime we will fix this function according to the values of the parameters m found in [92,93]

$$F(Q)\sim 1+4.981Q^{1.946}+0.127Q^{4.330}, \tag{4.10}$$

$$F(Q)\sim 1+0.335Q^{1.364}+0.0185Q^{2.315}, \tag{4.11}$$

$$F(Q)\sim\frac{1+0.4Q^{0.77}}{(1+0.15Q^{1.09})^2}, \tag{4.12}$$

$$F(Q)\sim 1, \tag{4.13}$$

for $m=3$, $m=1$, $m=-1$ and $m=0$, respectively. We can notice, from Eqs. (4.10)–(4.13), that in the strong dissipative regime, the scalar perturbations of the inflaton field will be enhanced for the case $m\neq 0$ as compared with the weak dissipative regime.

To complete the set of parameters required to constrain our model by the observational data, we introduce the amplitude of the tensor perturbation, P_T. As mentioned above, while the amplitude of the scalar perturbation in warm inflation is given by Eq. (4.3), the amplitude of the tensor perturbation remain unchanged and is given by [93]

$$P_T=2\kappa\left(\frac{H}{\pi}\right)^2, \tag{4.14}$$

and from Eq. (4.3), we can express the tensor-to-scalar ratio, $r=P_T/P_R$, in terms of the number of e-folds N as

$$r=\frac{8\kappa}{A^2f^2}\left[\frac{2Af(1-f)}{\kappa(1+Q)}\right]I(N)^{-f}(1-S(I(N))^{2f-2})\left(1+2n+\frac{2\sqrt{3}\pi Q}{\sqrt{3+4\pi Q}}\frac{T}{H}\right)^{-1}F(Q)^{-1}. \tag{4.15}$$

V. WEAK DISSIPATIVE REGIME

Considering that the system evolves according to the weak dissipative regime ($\Upsilon\ll 3H$). Performing the integration of Eq. (2.10), the evolution of the scalar field is given by

$$\begin{aligned}\phi_t-\phi_0&=\sqrt{\frac{8A(1-f)}{\kappa f}}t^{\frac{f}{2}}H_{A,f,c}(t),\\&=[\phi_t]_{\rm std}H_{A,f,c}(t),\end{aligned} \tag{5.1}$$

where the integration constant, ϕ_0, will be set to zero in the rest of the paper and $H_{A,f,c}(t)$, a correction term as compared to standard warm inflation [83], can be expressed as

$$H_{A,f,c}(t)={}_2F_1\left(-\frac{1}{2},\frac{f}{4(f-1)};\frac{5f-4}{4(f-1)};St^{2(f-1)}\right), \tag{5.2}$$

where ${}_2F_1(a,b;c;d)$ is the hypergeometric function and $S=\frac{3A^2f^2}{2\kappa\rho_c}$.

From Eqs. (3.1) and (2.18), as $Q=\Upsilon/3H\ll 1$, the dissipation coefficient Υ can be rewritten in terms of the scalar field as

$$\Upsilon=C_\phi^{\frac{4}{4-m}}\left[\frac{1-f}{2\kappa C_\gamma}\right]^{\frac{m}{4-m}}\phi^{\frac{4(1-m)}{4-m}}t^{-\frac{m}{4-m}}(1-St^{2f-2})^{\frac{m}{4-m}}. \tag{5.3}$$

The evolution of the scalar field and of the dissipation coefficient are given, respectively, at the horizon crossing t_k, by

$$\phi_{t_k}=\sqrt{\frac{8A(1-f)}{\kappa f}}(I(N))^{\frac{f}{2}}H_{A,f,c}(N) \tag{5.4}$$

and

$$\begin{aligned}\Upsilon=C_\phi^{\frac{4}{4-m}}&\left[\frac{1-f}{2\kappa C_\gamma}\right]^{\frac{m}{4-m}}\phi_{t_k}^{\frac{4(1-m)}{4-m}}(I(N))^{-\frac{m}{4-m}}\\&\times(1-S(I(N))^{2f-2})^{\frac{m}{4-m}}.\end{aligned} \tag{5.5}$$

If we compare the scalar field and the dissipation coefficient of our model at the horizon crossing with that

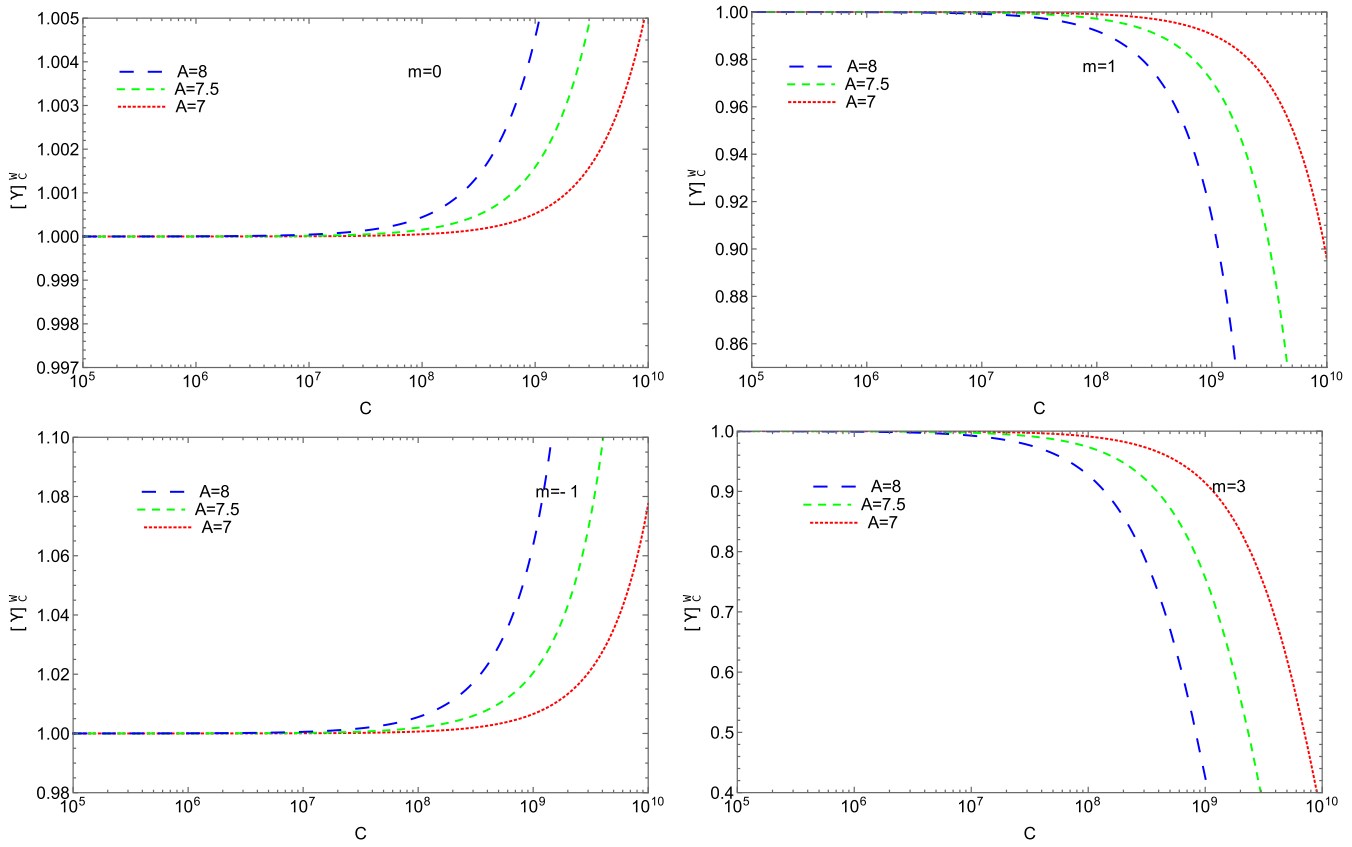

FIG. 3. Evolution of the correction term $[\Upsilon]_c^W$ versus the conformal anomaly coefficient c in the weak dissipative regime for $f = 0.125$ and for three different values of the parameter A, for the case $m = 0$ (upper left panel), $m = 1$ (upper right panel), $m = -1$ (lower left panel), and $m = 3$ (lower right panel). We have used $\kappa = 1$, $N = 60$, and $C_\gamma = 70$.

obtained in the case of standard warm inflation [83] we find, respectively,

$$\phi_{t_k} = [\phi_{t_k}]_{\rm std} H_{A,f,c}(N), \tag{5.6}$$

and

$$\Upsilon = [\Upsilon]_{\rm std}[\Upsilon]_c, \tag{5.7}$$

with

$$[\Upsilon]_{\rm std} = C_\phi^{\frac{4}{4-m}}\left[\frac{1-f}{2\kappa C_\gamma}\right]^{\frac{m}{4-m}} \phi_{\rm std}^{\frac{4(1-m)}{4-m}} (I(N))^{-\frac{m}{4-m}} \tag{5.8}$$

and

$$[\Upsilon]_c = (H_{A,f,c}(N))^{\frac{4(1-m)}{4-m}}(1 - S(I(N))^{2f-2})^{\frac{m}{4-m}}. \tag{5.9}$$

Here $H_{A,f,c}(N)$ and $[\Upsilon]_c$ represent corrections term to the scalar field and to the dissipation coefficient in the weak dissipation regime, respectively. We can show that the correction term $H_{A,f,c}(N)$ does not deviate too much from 1; i.e., the variation of the scalar field is not strongly affected by the AdS/CFT correspondence.

The dissipation term introduced previously in Eq. (2.5) describes the thermal radiation bath and its evolution versus the conformal anomaly coefficient tell us about the effect of AdS/CFT correspondence on the thermal process. From Fig. 3, we notice that the effect of the AdS/CFT correspondence is more significative and increases with the conformal anomaly coefficient for $c \geq 10^7$. This effect increases the thermal process. However, we can see from Eq. (5.5) that for specific values of A and f there must be a limiting value $S(I(N)) = 1$ beyond which the dissipation coefficient no longer makes sense.

To incorporate the observed parameters in warm inflation at the perturbative level, we rewrite the amplitude of the scalar perturbation Eqs. (4.7)–(4.9) and the tensor-to-scalar ratio Eq. (4.15) in the weak dissipative regime [(i.e., $F(Q) \simeq 1$] as follows:

$$P_R = \frac{A^4 f^4}{4\pi^2}\left[\frac{2Af(1-f)}{\kappa}\right]^{-1} I(N)^{3f-2}(1 - S(I(N))^{2f-2})^{-1}\left(1 + 2n + 2\pi Q\frac{T}{H}\right), \tag{5.10}$$

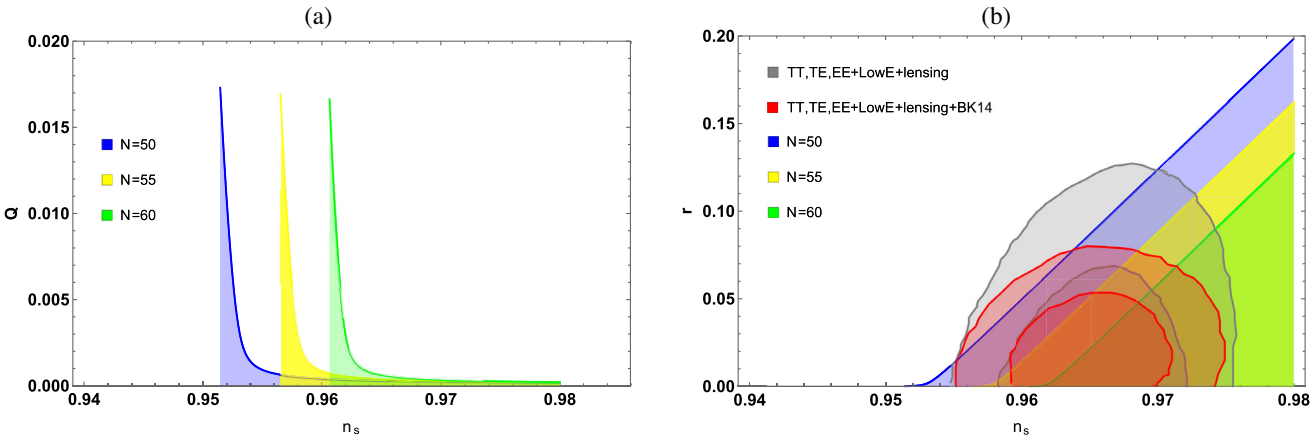

FIG. 4. The plots show the variation of the dissipative parameter Q (a) and the variation of the tensor-to-scalar ratio r (b) versus the spectral index n_s for different values of the e-fold number, the conformal anomaly coefficient $c = 10^7$ and the parameter $m = -1$. These plots are obtained for the following choice of parameters $C_\phi = 10^{-25}$, $0.1 < A < 2$, and $f = 0.125$.

$$\frac{T}{H} = \frac{1}{A.f}\left[\frac{3Af(1-f)}{2\kappa C_\gamma}Q\right]^{\frac{1}{4}} I(N)^{\frac{2-3f}{4}}(1 - S(I(N))^{2f-2})^{\frac{1}{4}}, \tag{5.11}$$

$$Q = \frac{C_\phi^{\frac{4}{4-m}}}{3Af}\left[\frac{(1-f)}{2\kappa C_\gamma}\right]^{\frac{m}{4-m}} \phi^{4\frac{1-m}{4-m}} I(N)^{-f+\frac{2m-4}{m-4}}[1 - S(I(N))^{2f-2}]^{\frac{m}{4-m}}, \tag{5.12}$$

$$r = \frac{8\kappa}{A^2 f^2}\left[\frac{2Af(1-f)}{\kappa}\right] I(N)^{-f}(1 - S(I(N))^{2f-2})\left(1 + 2n + 2\pi Q\frac{T}{H}\right)^{-1}, \tag{5.13}$$

where at the crossing horizon time, the inflaton field is given by Eqs. (5.1) and (6.2). Furthermore, by combining Eqs. (5.11) and (5.12), the above equations read

$$P_R = \frac{A^4 f^4}{4\pi^2}\left[\frac{2Af(1-f)}{\kappa}\right]^{-1} I(N)^{3f-2}(1 - S(I(N))^{2f-2})^{-1}\left(1 + 2n + 2\pi Q\frac{T}{H}\right), \tag{5.14}$$

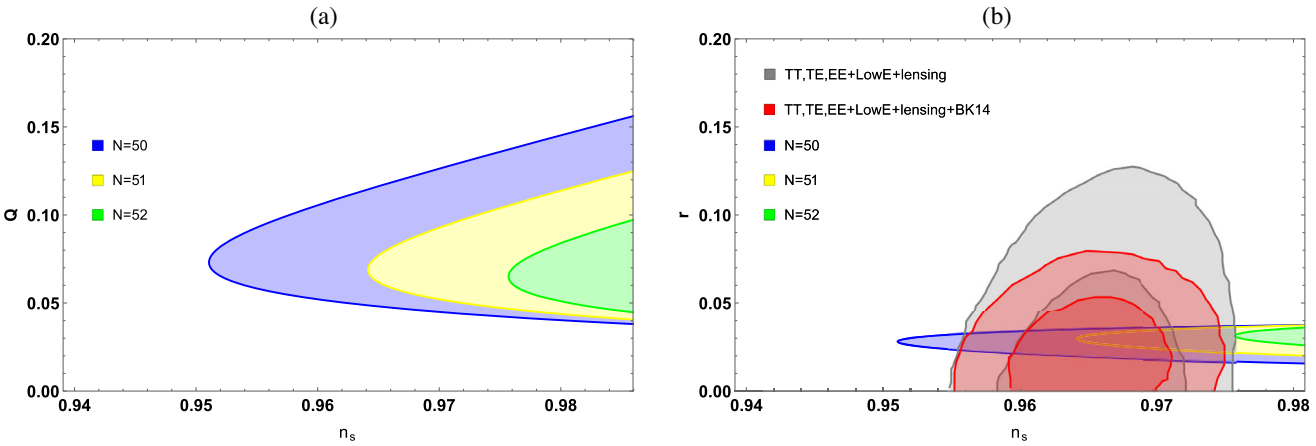

FIG. 5. The plots show the variation of the dissipative parameter Q (a) and the variation of the tensor-to-scalar ratio r (b) versus the spectral index n_s for different values of the e-fold number, the conformal anomaly coefficient $c = 10^7$ and the parameter $m = 3$. These plots are obtained for the following choice of parameters $C_\phi = 5.7 \times 10^7$, $0.1 < A < 0.5$, and $f = 0.5$.

$$\frac{T}{H}=\frac{1}{Af}\left[\frac{C_\phi(1-f)}{2\kappa C_\gamma}\right]^{\frac{1}{4-m}} I(N)^{-f+\frac{m-3}{m-4}}[1-S(I(N))^{2f-2}]^{\frac{1}{4-m}}\phi^{\frac{1-m}{4-m}}, \tag{5.15}$$

$$Q=\frac{C_\phi}{3Af}\left[\frac{C_\phi(1-f)}{2\kappa C_\gamma}\right]^{\frac{m}{4-m}}\phi^{4\frac{1-m}{4-m}} I(N)^{-f+\frac{2m-4}{m-4}}[1-S(I(N))^{2f-2}]^{\frac{m}{4-m}}, \tag{5.16}$$

$$r=\frac{8\kappa}{A^2f^2}\left[\frac{2Af(1-f)}{\kappa}\right] I(N)^{-f}(1-S(I(N))^{2f-2})\left(1+2n+2\pi Q\frac{T}{H}\right)^{-1}, \tag{5.17}$$

and the scalar spectral index $n_s=1-\frac{d\ln(P_R)}{dN}$ can be written as

$$\begin{aligned} n_s-1&=-(3f-2)\frac{d\ln I(N)}{dN}+\frac{d\ln(1-S(I(N))^{2f-2})}{dN}-\frac{d\ln\left(1+2n+2\pi Q\frac{T}{H}\right)}{dN},\\ &=-(3f-2)\frac{I(N)^{-f}}{Af}+\frac{2(1-f)SI(N)^{f-2}}{Af(1-S(I(N))^{2f-2})}+n_4, \end{aligned} \tag{5.18}$$

where we have used Eq. (3.7) and we have defined n_4 as

$$n_4=-\frac{d\ln\left(1+2n+2\pi Q\frac{T}{H}\right)}{dN}. \tag{5.19}$$

The term n_4 is obtained numerically. The numerical analysis is done for different values of the number of e-folds and the conformal anomaly coefficient is set to be $c=10^7$. We have also assumed the warm condition $(\frac{T}{H}>1)$, the weak dissipation case $(Q\ll 1)$ and we have constrained the spectral index in the observational range $0.9<n_s<1$.

The results show that the dissipative coefficients $\Upsilon_1=C_\phi T$ and $\Upsilon_0=C_\phi\phi$ are not supported by Planck data [14] for any set of values of C_ϕ, A, and f. However, for a convenient choice of those parameters, namely C_ϕ, A, and f, the dissipative coefficients $\Upsilon_{-1}=C_\phi\phi^2/T$ and $\Upsilon_3=C_\phi T^3/\phi^2$ are well supported by data. Indeed,

(i) For $m=-1$, we plot the dissipative parameter Q and the tensor-to-scalar ratio r as parametric functions of n_s for the following range of parameters $C_\phi=10^{-25}$, $0.1<A<2$, and $f=0.125$. The parametric plot is shown in Fig. 4.

(ii) For $m=3$, we plot the dissipative parameter Q and the tensor-to-scalar ratio r as parametric functions of n_s for the following range of parameters $C_\phi=5.7\times 10^7$, $0.1<A<0.5$, and $f=0.5$. The parametric plot is shown in Fig. 5.

We notice from the plots of Figs. 4 and 5, that we are, indeed, in the weak dissipative regime. From the plots of the same Fig. 4, i.e., $m=-1$ and $m=3$ in the dissipative coefficient, we notice that the tensor-to-scalar ratio lies in the 1σ contour of Planck data for $N=55$ and $N=60$. This means that the weak dissipative regime in warm inflation in the holographic context under consideration may reproduce the observational data for the choice of parameters considered above.

VI. STRONG DISSIPATIVE REGIME $\Upsilon\gg 3H$

In this section, we analyze the strong dissipative regime, $(Q\gg 1)$, by considering exact solutions for the cases $m=3$ and $m\neq 3$. When integrating Eq. (2.10) by using Eq. (3.1), the evolution of the scalar field is given by

$$\phi_t-\phi_0=\begin{cases}\left[\frac{(3-m)G_m(t)}{2K_m}\right]^{\frac{2}{3-m}}, & \text{for } m\neq 3\\ \exp\left[\frac{G_m(t)}{K_m}\right], & \text{for } m=3\end{cases}, \tag{6.1}$$

with

$$G_m(t)=H^s_{A,f,c,m}(t)t^{\frac{(8-m)f+2(m-2)}{8}}, \tag{6.2}$$

$$H^s_{A,f,c,m}(t)={}_2F_1\left(\frac{m-4}{8},\frac{(8-m)f+2(m-2)}{16(f-1)};1+\frac{(8-m)f+2(m-2)}{16(f-1)};St^{2(f-1)}\right), \tag{6.3}$$

$$K_m=\left(\frac{(8-m)f+2(m-2)}{8}\right)\left(\frac{4AfC_\gamma}{C_\phi}\right)^{-\frac{1}{2}}\left(\frac{3Af(1-f)}{2\kappa C_\gamma}\right)^{\frac{m-4}{8}}, \tag{6.4}$$

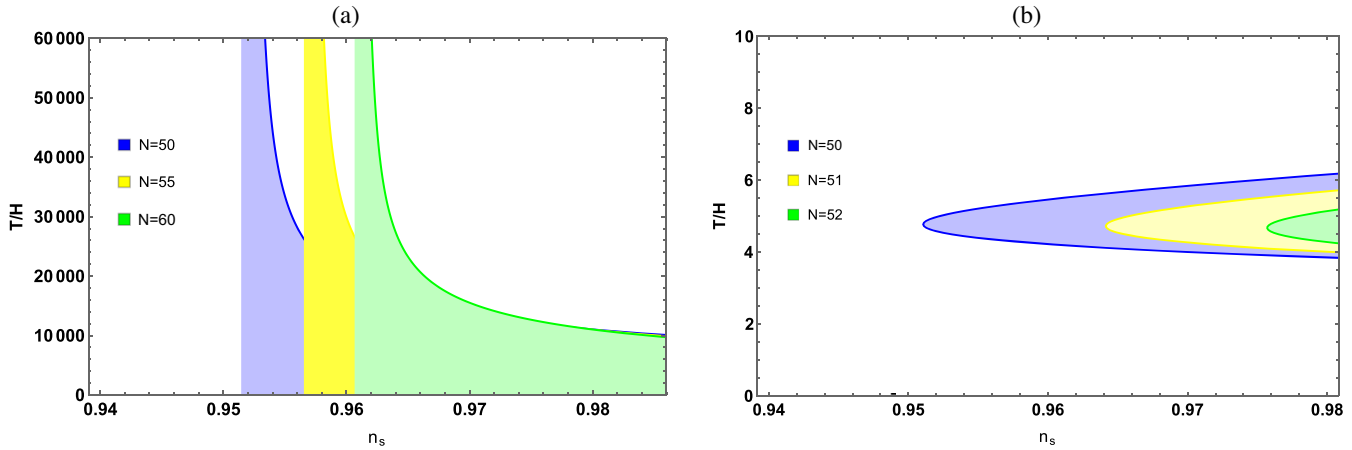

FIG. 6. The value of T/H versus the spectral index n_s for the conformal anomaly coefficient $c = 10^7$ for the $m = -1$, $C_\phi = 10^{-25}$ curve (a) and for the $m = 3$, $C_\phi = 5.7 \times 10^7$ curve (b).

where ϕ_0 is an integration constant that will be set to $\phi_0 = 0$ in the rest of the paper, $H^s_{A,f,c,m}(t)$, is a correction term to standard warm inflation, and $S = \frac{3A^2f^2}{2\kappa\rho_c}$.

Since $Q = \Upsilon/3H \gg 1$ and using Eqs. (2.18) and (3.1), the dissipation coefficient Υ can be rewritten in terms of the scalar field as

$$\Upsilon = C_\phi \left[\frac{-3Af(f-1)}{2\kappa C_\gamma}\right]^{\frac{m}{4}} t^{\frac{m}{4}(f-2)} \phi^{1-m} (1 - St^{2(f-1)})^{\frac{m}{4}}. \quad (6.5)$$

If we compare the amplitude of the scalar inflaton field Eq. (6.1) and the dissipation coefficient Eq. (6.5) at the horizon crossing and for $m \neq 3$ with that obtained in the case of standard warm inflation (see Ref. [83]), then we find, respectively, that

$$\phi_{t_k} = [\phi_{t_k}]_{\rm std} (H^s_{A,f,c,m}(N))^{\frac{2}{3-m}} \quad (6.6)$$

and

$$\Upsilon = [\Upsilon]_{\rm std} [\Upsilon]^s_c, \quad (6.7)$$

with

$$[\Upsilon]^s_c = (H^s_{A,f,c,m}(N))^{2\frac{(1-m)}{(3-m)}} (1 - St_k^{2f-2})^{\frac{m}{4}}, \quad (6.8)$$

is the correction term of the dissipation coefficient in the strong dissipation regime.

Figure 6 shows the plot of T/H versus the spectral index in the weak dissipation regime for $m = -1$ [Fig. 6(a)] and $m = 3$ [Fig. 6(b)]. Figures 6(a) and 6(b) are obtained for the same choice of parameters as in Figs. 5(a) and 5(b), respectively. These figures show clearly that the results obtained in Fig. 5 satisfy the warm condition.

Figure 7 shows the evolution of the correction term $[\Upsilon]^s_c$ versus the conformal anomaly coefficient c for three values of the parameter m and for a fixed value of the parameter $f = 0.25$ and for three values of the parameter A. We notice that the AdS/CFT correspondence has no significant effect and the thermal process is described by standard warm inflation for $c < 10^7$ for the three chosen values of m parameters. Furthermore, while for $m = 0$ and $m = 1$ the thermal process decreases, it increases strongly for $m = -1$ with the increasing values of the conformal anomaly coefficient $c > 10^7$ for the range of f and A considered. However this range of the conformal anomaly may change by changing the value of f and A.

Furthermore, in the strong dissipative regime, $1 \ll Q$, Eqs. (4.7)–(4.9) and (4.15) take the following forms:

$$P_R = \frac{\sqrt{3\pi}A^2f^2\kappa}{8\pi^2(1-f)} \left[\frac{3Af(1-f)}{2\kappa C_\gamma}\right]^{\frac{1}{4}} I(N)^{\frac{3(3f-2)}{4}} (1 - S(I(N))^{2f-2})^{-\frac{3}{4}} Q^{\frac{3}{2}} F(Q), \quad (6.9)$$

$$\frac{T}{H} = \frac{1}{Af} \left[\frac{3Af(1-f)}{2\kappa C_\gamma}\right]^{\frac{1}{4}} I(N)^{\frac{2-3f}{4}} (1 - S(I(N))^{2f-2})^{\frac{1}{4}}, \quad (6.10)$$

$$Q = C_\phi [3Af]^{\frac{4}{4-m}} \left[\frac{(1-f)}{2\kappa C_\gamma}\right]^{\frac{m}{4}} I(N)^{f\frac{(m-4)}{4} + \frac{m-2}{2}} [1 - S(I(N))^{2f-2}]^{\frac{m}{4}} \phi^{1-m}, \quad (6.11)$$

$$r = \frac{16(1-f)}{\sqrt{3\pi}} \left[\frac{3Af(1-f)}{2\kappa C_\gamma}\right]^{-\frac{1}{4}} I(N)^{-\frac{(f+2)}{4}} (1 - S(I(N))^{2f-2})^{\frac{3}{4}} Q^{-\frac{3}{2}} F(Q)^{-1}. \quad (6.12)$$

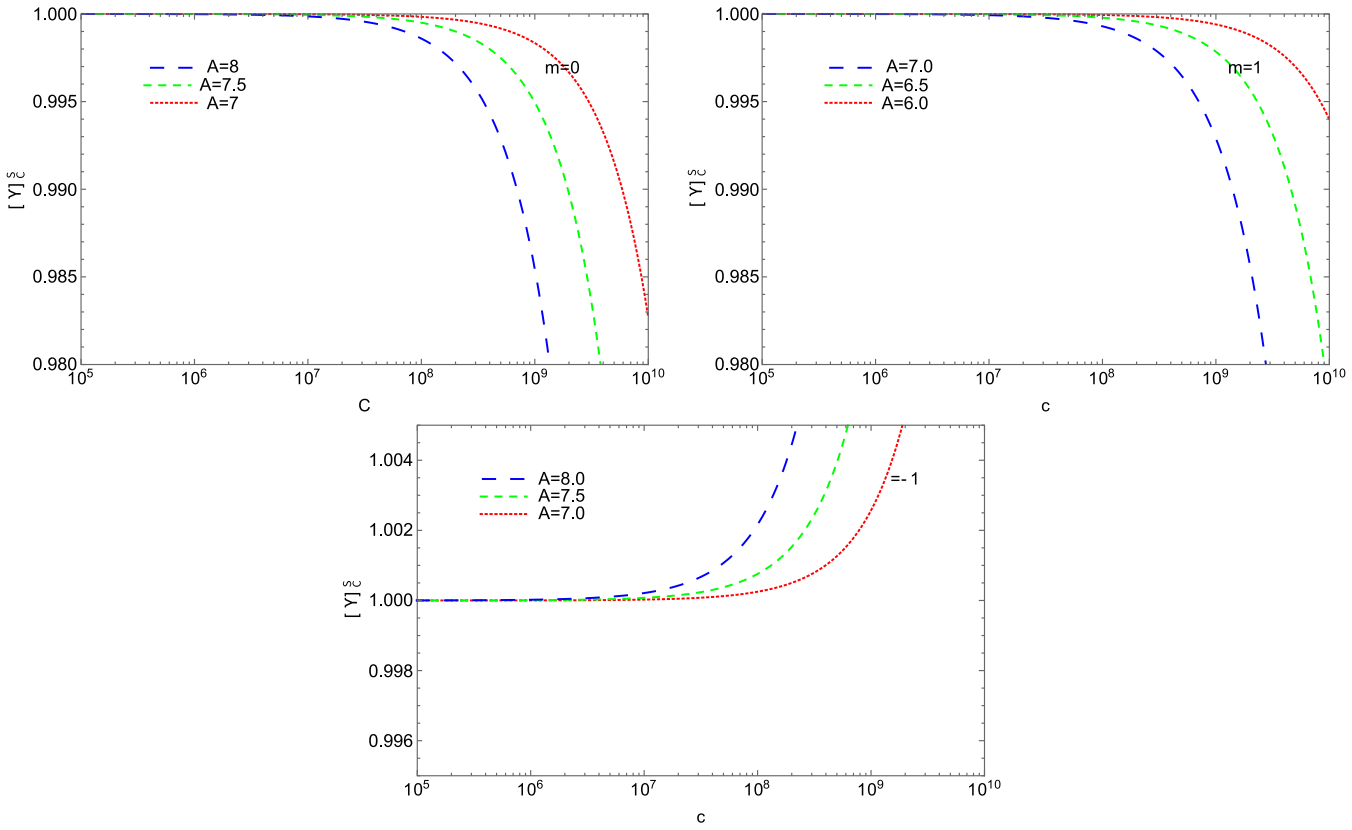

FIG. 7. Evolution of the correction term $[\Upsilon]_c^s$ versus the conformal anomaly coefficient c for $f = 0.125$ and for different values of the parameter A for the cases $m = 0$ (upper left panel), $m = 1$ (upper right panel), and $m = -1$ (lower panel), we have used, $\kappa = 1$, $N = 60$, and $C_\gamma = 70$.

We notice here that $\frac{T}{H}$ in Eq. (6.10) is independent of the parameters Q, m, and C_ϕ. We notice also that according to the function $F(Q)$, which characterizes the coupling between the inflaton field and radiation, Eqs. (4.10)–(4.12), and Eqs. (6.9) and (6.11) that a strong effect is observed on the amplitude of the scalar perturbation in the strong dissipative regime particularly in the case of $m \neq 0$.

As in the weak dissipation case, a numerical approach to calculate the scalar spectral index $n_s = 1 - \frac{d\ln(P_R)}{dN}$ is mandatory. To this aim, we set the value of the conformal anomaly coefficient to $c = 10^7$, we consider as well the

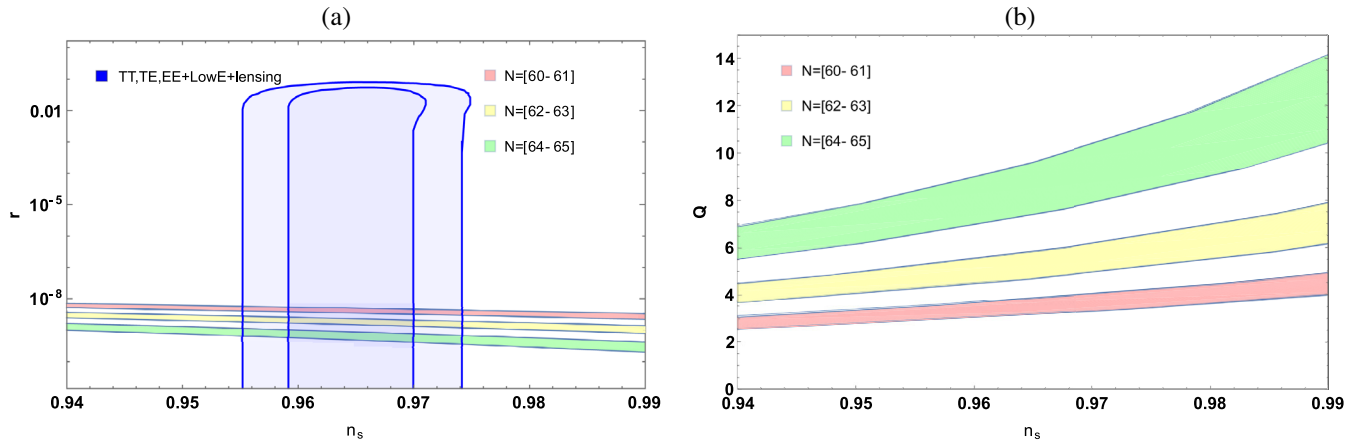

FIG. 8. The plots show the variation of the dissipative parameter Q (a) and the variation of the tensor-to-scalar ratio r (b) versus the spectral index n_s for different values of the e-fold number, the conformal anomaly coefficient $c = 10^7$ and the parameter $m = 1$. These plots are obtained for the following choice of parameters $C_\phi = 10^{10}$, $0.1 < A < 6$, and $f = 0.0625$.

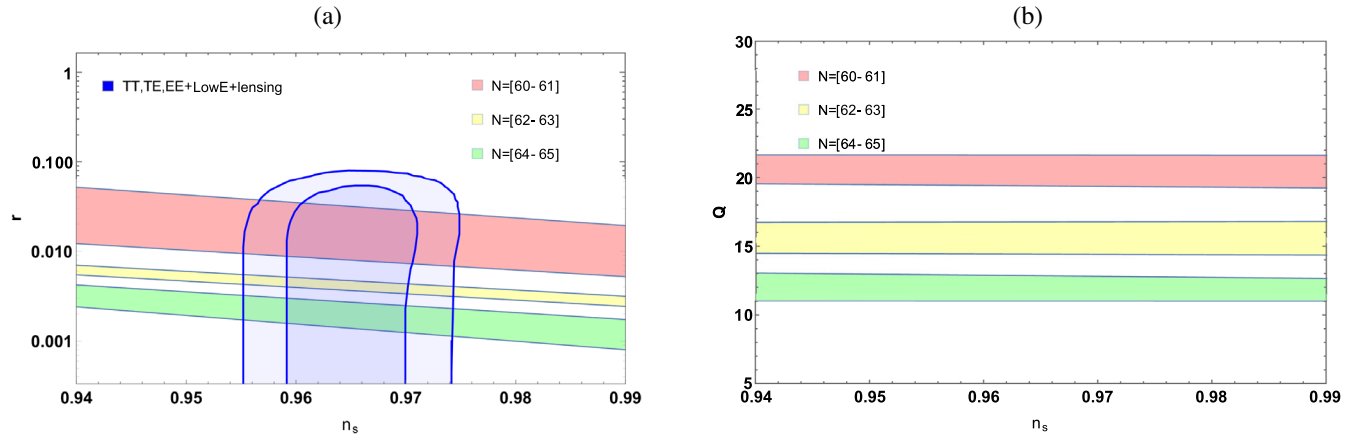

FIG. 9. The plots show the variation of the dissipative parameter Q (a) and the variation of the tensor-to-scalar ratio r (b) versus the spectral index n_s for different values of the e-fold number, the conformal anomaly coefficient $c = 10^7$ and the parameter $m = 3$. These plots are obtained for the following choice of parameters $C_\phi = 1.5 \times 10^5$, $0.1 < A < 4$, and $f = 0.25$.

warm condition $(\frac{T}{H} > 1)$ and the strong dissipation case $(Q \gg 1)$.

The results show that, for any range of parameters C_ϕ, A, and f, the dissipative coefficient Υ_1 and Υ_0 are excluded by observational data. We plot the dissipative parameters and the tensor-to-scalar ratio (Q and r) as parametric functions of the spectral index n_s. For the dissipative parameter Q, Fig. 8, the range of parameters considered are $C_\phi = 10^{10}$, $0.1 < A < 6$, and $f = 0.0625$. While for the dissipative parameter Q, Fig. 9, the range of parameters considered are $C_\phi = 1.5 \times 10^5$, $0.1 < A < 4$, and $f = 0.25$. We notice from the plots of Figs. 8 and 9, that we are, indeed, in the strong dissipative regime. For the plots of the same Figs. 8 and 9, i.e., $m = 1$ and $m = 3$ in the dissipative coefficient, we notice that the tensor-to-scalar ratio and the spectral index values agrees with the 1σ contour of Plank data for a large values of N e-folds. In Fig. 10 we show the evolution of T/H versus the spectral index in the strong regime for $c = 10^7$, $0.1 < A < 6$, and $f = 0.25$. The curve confirms that the result obtained in the strong dissipation regime satisfy the conditions of warm inflation. This means that the strong dissipative regime of warm inflation in the holographic context under consideration is in agreement with the observational data for the choice of parameters mentioned above.

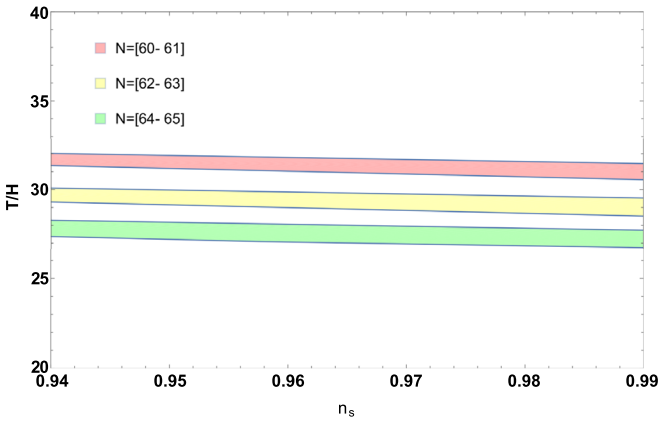

FIG. 10. The strong dissipation regime value of T/H versus the spectral index for the conformal anomaly coefficient $c = 10^7$, $0.1 < A < 6$, and $f = 0.25$.

VII. CONCLUSIONS

In this work, we have studied warm inflation with a scalar field in the context of the AdS/CFT correspondence and with a general form for the dissipative coefficient. We have considered that the scale factor evolve with time during intermediate inflation as $a(t) = a_I \exp At^f$, $(0 < f < 1)$. In this context, we have provided the basic equation in the weak and the strong dissipation regime and we have shown that these equations are equal to the standard one times some corrections term which at the low energy limit tends to one. We have discussed our model in the frame of warm inflation condition $(T/H > 1)$ by determining the consistent range of C_ϕ parameter of the dissipative coefficent, A and f parameters of the intermediate inflation (see Figs. 4, 5, 8, and 9).

We have examined our theoretical prediction by plotting the evolution of different inflationary parameters versus observational data. In both dissipative regimes, while our model is well supported by Planck data for the dissipative coefficient Υ_3, it is not the case for the dissipative coefficient Υ_0. However, while the dissipative coefficient Υ_{-1} is well supported by Planck data in the weak dissipative regime, the dissipative coefficient Υ_1 is well supported in the strong dissipative regime.

We have shown that for a suitable interval of C_ϕ parameters of the dissipative coefficient and for A and f parameters of the intermediate inflation our predicted inflationary parameters are consistent with the 1σ confidence level contours derived from Planck data.

Finally, we conclude that scalar warm inflation in the context of holographic cosmology for the cases $m = -1$, $m = 1$ and $m = 3$ may describe the inflationary era and predicts the appropriate inflationary parameters with respect to the observational data within a slow roll approximation for the weak, strong, and both regime, respectively.

ACKNOWLEDGMENTS

We thank the referee for her/his suggestion concerning the perturbation issue. The work of M. B. L. is supported by the Basque Foundation of Science Ikerbasque. She also would like to acknowledge the support from the Basque government Grant No. IT956-16 (Spain) and from the Grant No. PID2020–114035 GB-100, funded by MCIN/638AEI/10.13039/501100011033 and by "ERDF A way of making Europe." She is also partially supported by the Grant FIS2017-85076-P, funded by MCIN/638AEI/10.13039/501100011033 and by "ERDF A way of making Europe."

[1] A. A. Starobinsky, Phys. Lett. **91B**, 99 (1980).
[2] A. D. Linde, Phys. Lett. **129B**, 177 (1983).
[3] K. Sato, Mon. Not. R. Astron. Soc. **195**, 467 (1981).
[4] A. D. Linde, Phys. Lett. **108B**, 389 (1982).
[5] A. H. Guth, Phys. Rev. D **23**, 347 (1981).
[6] A. Albrecht and P. J. Steinhardt, Phys. Rev. Lett. **48**, 1220 (1982); A. Linde, *Particle Physics and Inflationary Cosmology* (Gordon and Breach, New York, 1990).
[7] V. F. Mukhanov and G. V. Chibisov, Pis'ma Zh. Eksp. Teor. Fiz. **33**, 549 (1981) [JETP Lett. **33**, 532 (1981)].
[8] S. W. Hawking, Phys. Lett. **115B**, 295 (1982).
[9] A. H. Guth and S.-Y. Pi, Phys. Rev. Lett. **49**, 1110 (1982).
[10] A. A. Starobinsky, Phys. Lett. **117B**, 175 (1982).
[11] J. M. Bardeen, P. J. Steinhardt, and M. S. Turner, Phys. Rev. D **28**, 679 (1983).
[12] C. L. Bennett *et al.*, Astrophys. J. Suppl. Ser. **192**, 17 (2011).
[13] G. Hinshaw *et al.* (WMAP Collaboration), Astrophys. J. Suppl. Ser. **208**, 19 (2013).
[14] P. A. R. Ade *et al.* (Planck Collaboration), Astron. Astrophys. **594**, A13 (2016).
[15] E. Komatsu *et al.* (WMAP Collaboration), Astrophys. J. Suppl. Ser. **192**, 18 (2011); B. Gold *et al.*, Astrophys. J. Suppl. Ser. **192**, 15 (2011).
[16] D. Larson *et al.*, Astrophys. J. Suppl. Ser. **192**, 16 (2011).
[17] J. Khoury, B. A. Ovrut, P. J. Steinhardt, and N. Turok, Phys. Rev. D **64**, 123522 (2001); P. J. Steinhardt and N. Turok, Science **296**, 1436 (2002).
[18] F. Finelli and R. Brandenberger, Phys. Rev. D **65**, 103522 (2002).
[19] M. Gasperini and G. Veneziano, Astropart. Phys. **1**, 317 (1993).
[20] A. Nayeri, R. H. Brandenberger, and C. Vafa, Phys. Rev. Lett. **97**, 021302 (2006); R. H. Brandenberger, A. Nayeri, S. P. Patil, and C. Vafa, Phys. Rev. Lett. **98**, 231302 (2007).
[21] K. Hinterbichler and J. Khoury, J. Cosmol. Astropart. Phys. 04 (2012) 023.
[22] A. Berera, Phys. Rev. D **55**, 3346 (1997).
[23] A. Berera, Phys. Rev. Lett. **75**, 3218 (1995).
[24] L. M. H. Hall, I. G. Moss, and A. Berera, Phys. Rev. D **69**, 083525 (2004).
[25] I. G. Moss, Phys. Lett. **154B**, 120 (1985).
[26] A. Berera and L. Z. Fang, Phys. Rev. Lett. **74**, 1912 (1995).
[27] A. Berera, Nucl. Phys. **B585**, 666 (2000).
[28] A. Berera, Phys. Rev. D **54**, 2519 (1996).
[29] A. Berera, I. G. Moss, and R. O. Ramos, Rep. Prog. Phys. **72**, 026901 (2009).
[30] M. Bastero-Gil and A. Berera, Int. J. Mod. Phys. A **24**, 2207 (2009).
[31] E. D. Stewart, Phys. Rev. D **51**, 6847 (1995).
[32] G. R. Dvali and S. H. H. Tye, Phys. Lett. B **450**, 72 (1999).
[33] V. Kamali, M. Motaharfar, and R. O. Ramos, Phys. Rev. D **101**, 023535 (2020).
[34] R. Herrera, N. Videla, and M. Olivares, Eur. Phys. J. C **75**, 205 (2015).
[35] R. Herrera, N. Videla, and M. Olivares, Phys. Rev. D **90**, 103502 (2014).
[36] M. Bastero-Gil, A. Berera, and J. G. Rosa, Phys. Rev. D **84**, 103503 (2011).
[37] J. M. Romero and M. Bellini, Phys. Lett. B **669**, 1 (2009).
[38] K. Nozari, M. Shoukrani, and B. Fazlpour, Gen. Relativ. Gravit. **43**, 207 (2011).
[39] A. Deshamukhya and S. Panda, Int. J. Mod. Phys. D **18**, 2093 (2009).
[40] M. A. Cid, S. del Campo, and R. Herrera, J. Cosmol. Astropart. Phys. 10 (2007) 005.
[41] S. del Campo and R. Herrera, Phys. Lett. B **653**, 122 (2007).
[42] M. A. Cid, S. del Campo, and R. Herrera, J. Cosmol. Astropart. Phys. 10 (2007) 005.
[43] R. Herrera, Phys. Rev. D **81**, 123511 (2010).
[44] X.-M. Zhang and J.-Y. Zhu, Phys. Rev. D **87**, 043522 (2013).
[45] R. Herrera, M. Olivares, and N. Videla, Int. J. Mod. Phys. D **23**, 1450080 (2014).
[46] L. L. Graef and R. O. Ramos, Phys. Rev. D **98**, 023531 (2018).
[47] M. Benetti, L. Graef, and R. O. Ramos, J. Cosmol. Astropart. Phys. 10 (2019) 066.

[48] L. Randall and R. Sundrum, Phys. Rev. Lett. **83**, 4690 (1999).
[49] J. M. Maldacena, Adv. Theor. Math. Phys. **2**, 231 (1998); Int. J. Theor. Phys. **38**, 1113 (1999).
[50] J. E. Lidsey and D. Seery, Phys. Rev. D **73**, 023516 (2006).
[51] Z. Bouabdallaoui, A. Errahmani, M. Bouhmadi-López, and T. Ouali, Phys. Rev. D **94**, 123508 (2016).
[52] A. Bargach, F. Bargach, and T. Ouali, Nucl. Phys. **B940**, 10 (2019).
[53] A. Bargach, F. Bargach, A. Errahmani, and T. Ouali, Int. J. Mod. Phys. D **29**, 2050010 (2020).
[54] A. Bargach, F. Bargach, M. Bouhmadi-López, and T. Ouali, Phys. Rev. D **102**, 123540 (2020).
[55] J. D Barrow and A. R. Liddle, Phys. Rev. D **47**, R5219 (1993).
[56] J. D. Barrow and N. J. Nunes, Phys. Rev. D **76**, 043501 (2007).
[57] R. Herrera and N. Videla, Eur. Phys. J. C **67**, 499 (2010).
[58] R. Herrera, M. Olivares, and N. Videla, Eur. Phys. J. C **73**, 2295 (2013).
[59] R. Herrera, M. Olivares, and N. Videla, Eur. Phys. J. C **73**, 2475 (2013).
[60] R. Herrera and E. San Martin, Eur. Phys. J. C **71**, 1701 (2011).
[61] E. Kiritsis, J. Cosmol. Astropart. Phys. 10 (2005) 014.
[62] I. G. Moss and C. Xiong, Gen. Relativ. Gravit. **38**, 12091213 (2006), arXiv:hep/0603266.
[63] M. Gleiser and R. O. Ramos, Phys. Rev. D **50**, 2441 (1994).
[64] A. Berera, M. Gleiser, and R. O. Ramos, Phys. Rev. D **58**, 123508 (1998).
[65] A. Berera and R. O. Ramos, Phys. Rev. D **63**, 103509 (2001).
[66] Y. Zhang, J. Cosmol. Astropart. Phys. 03 (2009) 023.
[67] M. Bastero-Gil, A. Berera, and R. O. Ramos, J. Cosmol. Astropart. Phys. 07 (2011) 030.
[68] M. Bastero-Gil, A. Berera, R. O. Ramos, and J. G. Rosa, J. Cosmol. Astropart. Phys. 01 (2013) 016.
[69] H. P. de Oliveira and R. O. Ramos, Phys. Rev. D **57**, 741 (1998).
[70] I. G. Moss and C. Xiong, J. Cosmol. Astropart. Phys. 11 (2008) 023.
[71] G. Panotopoulos and N. Videla, Eur. Phys. J. C **75**, 525 (2015).
[72] M. Bastero-Gil, A. Berera, R. O. Ramos, and J. G. Rosa, Phys. Rev. Lett. **117**, 151301 (2016).
[73] M. Bastero-Gil, A. Berera, and R. O. Ramos, J. Cosmol. Astropart. Phys. 09 (2011) 033.
[74] K. V. Berghaus, P. W. Graham, and D. E. Kaplan, J. Cosmol. Astropart. Phys. 03 (2020) 034.
[75] M. Laine and S. Procacci, J. Cosmol. Astropart. Phys. 06 (2021) 031.
[76] M. Motaharfar and R. O. Ramos, Phys. Rev. D **104**, 043522 (2021).
[77] M. Bastero-Gil, A. Berera, R. O. Ramos, and J. G. Rosa, Phys. Lett. B **813**, 136055 (2021).
[78] W. DeRocco, P. W. Graham, and S. Kalia, J. Cosmol. Astropart. Phys. 11 (2021) 011.
[79] J. C. B. Sanchez, M. Bastero-Gil, A. Berera, and K. Dimopoulos, Phys. Rev. D **77**, 123527 (2008).
[80] R. O. Ramos and L. A. da Silva, J. Cosmol. Astropart. Phys. 03 (2013) 032.
[81] R. Cerezo and J. G. Roza, J. High Energy Phys. 01 (2013) 024.
[82] S. Das and R. O. Ramos, Phys. Rev. D **102**, 103522 (2020).
[83] R. Herrera, M. Olivares, and N. Videla, Phys. Rev. D **88**, 063535 (2013).
[84] E. W. Kolb and M. S. Turner, Front. Phys. **69**, 1 (1990).
[85] F. Lucchin and S. Matarrese, Phys. Rev. D **32**, 1316 (1985).
[86] M. Bouhmadi-López, A. Errahmani, P. Martín-Moruno, T. Ouali, and Y. Tavakoli, Int. J. Mod. Phys. D **24**, 1550078 (2015).
[87] J. Martin, C. Ringeval, and V. Vennin, Phys. Dark Universe **5–6**, 75 (2014).
[88] M. Bastero-Gil, A. Berera, I. G. Moss, and R. O. Ramos, J. Cosmol. Astropart. Phys. 05 (2014) 004.
[89] M. Bastero-Gil, A. Berera, I. G. Moss, and R. O. Ramos, J. Cosmol. Astropart. Phys. 12 (2014) 008.
[90] C. Graham and I. G. Moss, J. Cosmol. Astropart. Phys. 07 (2009) 013.
[91] S. Bartrum, M. Bastero-Gil, A. Berera, R. Cerezo, R. O. Ramos, and J. G. Rosa, Phys. Lett. B **732**, 116 (2014).
[92] M. Benetti and R. O. Ramos, Phys. Rev. D **95**, 023517 (2017).
[93] M. Motaharfar, V. Kamali, and R. O. Ramos, Phys. Rev. D **99**, 063513 (2019).